

QUARTIC FORMULATION FOR ELASTIC BEAM-COLUMNS SUBJECT TO THERMAL EFFECTS

B.A. Izzuddin¹

ABSTRACT

This paper presents an advanced elastic formulation intended for modelling imperfect beam-columns subject to thermal loading using only one element per member. The new formulation is derived in a local Eulerian (convected) system, where the effects of large displacements and rotations in three-dimensional space are accounted for through transformations between the local and global systems. In the Eulerian system, the proposed formulation utilises quartic shape functions for the transverse displacements and linear shape functions for the rotational twist, whereas no shape functions are required for the axial displacement since the constant axial force criterion is used. The paper proceeds with providing the formulation details, where particular emphasis is placed on the modelling of thermal effects. This is followed by a discussion on the modelling of distributed element loads which require special treatment in the context of the large displacement Eulerian approach. Finally, verification of the new formulation is undertaken using the nonlinear analysis program ADAPTIC, where several examples are presented to illustrate the accuracy and efficiency of the quartic formulation.

KEYWORDS

Nonlinear analysis. Beam-column formulation. Thermal effects. Steel frames.

¹ Lecturer in Engineering Computing, Civil Engineering Department, Imperial College, London SW7 2BU, U.K.

INTRODUCTION

Recent years have witnessed increasing research into the behaviour of structural frames under fire conditions, particularly addressing issues related to the interaction between structural members which are affected by fire and other structural members, and the influence of this interaction on the fire resistance of the overall structure. Typically for steel frames, fire loading is associated with thermal and plastic strains as well as changes in the material properties, including reduction in both the elastic modulus and the yield strength of steel.

The case for an elastic formulation capable of modelling the geometrically nonlinear response of imperfect beam-columns under thermal loading is made here on two grounds. Firstly, considering steel for example, there is a wide range of temperature variation to which correspond considerable thermal strains and reduction in the elastic modulus with insignificant variation in the yield strength. As a result, for many structural frames a moderate increase in temperatures could easily initiate elastic instability, particularly if the affected members are subject to significant compressive axial forces. Secondly, even when the structural resistance is governed by elasto-plastic behaviour, adaptive elasto-plastic thermal analysis (Izzuddin *et al.*, 1995) utilises, and indeed requires the use of, an accurate elastic nonlinear formulation capable of representing an entire member with only one element. In essence, the adaptive elasto-plastic technique, developed by the author for steel frames (Izzuddin, 1991; Izzuddin & Elnashai, 1993-a) and extended recently to reinforced concrete frames (Izzuddin *et al.*, 1994; Karayannis *et al.*, 1994), starts the analysis using one elastic nonlinear element per member. During analysis, the adaptive procedure monitors the various elastic elements for occurrence of material plasticity, and modifies the element mesh by introducing elasto-plastic elements in those regions which develop material plasticity. By using the more computationally expensive elasto-plastic elements only *when* and *where* necessary, within the structure and during analysis respectively, adaptive elasto-plastic analysis achieves considerable modelling advantages and computational savings often in excess of 80%.

Extensive research efforts have been devoted over the past few years to the development of advanced methods for the large displacement geometrically nonlinear analysis of framed structures

(Oran, 1973; Kondoh *et al.*, 1986; Kassimali & Abbasnia, 1990; Izzuddin & Elnashai, 1993-b). These developments have been accompanied by research into formulations capable of representing a whole member with only one element, mainly driven by the computational savings and modelling advantages that could be derived. Soreide *et al.* (1987) presented a beam-column formulation employing trigonometric shape functions which are dependent on the unknown axial force, thus requiring an iterative procedure on the element level to establish the element deformed shape and its nodal forces including the axial force. Al-Bermani and Kitipornchai (1990) derived a deformation matrix accounting for the coupling between axial deformation on the one hand and the lateral and torsional deformation on the other to model the beam-column effect as well as axial-torsional coupling of a whole member using one element. So and Chan (1991) presented a quartic formulation and suggested its applicability to the modelling of beam-columns using only one element per member, even though their formulation overestimates the post-buckling response considerably. Izzuddin and Elnashai (1994) attributed this inaccuracy to the use of a linear shape function for the axial displacements, and the authors pointed out that a quartic formulation employing the constant axial force criterion (Izzuddin, 1991) predicts the post-buckling response more accurately.

This paper presents a new formulation aimed at modelling the large displacement response of imperfect beam-columns subject to thermal effects using only one element per member. A local Eulerian system is used to derive the formulation details, with transformations between the local Eulerian system and the global system employed to account for large global displacements and finite rotations (Izzuddin & Elnashai, 1993-b). The proposed formulation extends the aforementioned quartic beam-column element developed by the author (Izzuddin, 1991) to include thermal effects in the geometrically nonlinear range and the modelling of distributed loading. With regard to the former point, the effects of both thermal strains and the reduction in the elastic modulus at elevated temperatures are included. For the latter point, a special treatment of distributed loading is suggested, particularly in view of the complexity of modelling accurately such loads within an Eulerian large displacement approach. This complexity was pointed out by Oran and Kassimali (1976) in the context of dynamic analysis employing distributed mass representation.

The paper proceeds by providing the quartic formulation details, with particular emphasis placed on the modelling of thermal effects. Verification of the formulation is undertaken using the nonlinear analysis program ADAPTIC (Izzuddin, 1991; Izzuddin & Elnashai, 1992), where several examples are used to demonstrate the formulation accuracy and efficiency.

FORMULATION DETAILS

Basic Assumptions

In the development of the quartic beam-column formulation, the following simplifying assumptions are made:

1. Plane sections remain plane upon deformation.
2. Shear strains due to flexure are negligible.
3. Warping strains due to non-uniform torsion are negligible.
4. The cross-sectional centroid and shear centre are coincident.
5. The elastic moduli are uniform over the cross-section.

With these assumptions, the strain state of a cross-section can be completely defined by means of four generalised strains $(\epsilon_c, \kappa_y, \kappa_z, \xi)$, representing the centroidal axial strain, curvatures about the cross-sectional principal axes and specific twist, respectively, thus allowing a one-dimensional formulation to be adopted. The corresponding four generalised stresses (f, m_y, m_z, m_T) , representing the axial force, biaxial bending moments and torque, respectively, can then be obtained as:

$$f = EA (\epsilon_c - \epsilon_c^t) \quad (1.a)$$

$$m_y = EI_y (\kappa_y - \kappa_y^t) \quad (1.b)$$

$$m_z = EI_z (\kappa_z - \kappa_z^t) \quad (1.c)$$

$$m_T = GJ \xi \quad (1.d)$$

where,

E:	Young's elastic modulus
G:	Elastic shear modulus
A:	Cross-sectional area
I_y, I_z :	Second moments of area about principal axes
J:	St. Venant's torsion constant
$\varepsilon_c^t, \kappa_y^t, \kappa_z^t$:	Generalised thermal strains.

Although in (1) the elastic moduli (E) and (G) are assumed uniform over the cross-section, their variation along the element length, which may be due to varying temperatures, will be accounted for. Taking steel for example, the effect of elevated temperatures on (E) becomes significant after a threshold temperature (t_s) has been exceeded (Cooke, 1988; EC3, 1993), as illustrated in Fig. 1. With the assumption that (E) is uniform over the cross-section, one of the following two conditions must be satisfied:

1. Temperature can vary within the cross-section but is less than (t_s)
2. Temperature is uniform over the cross-section.

If both conditions are violated considerably, the proposed quartic formulation becomes inaccurate, in which case more sophisticated elements accounting for the variation of (E) over the cross-section would be needed. However, in the context of adaptive analysis (Izzuddin & Elnashai, 1993-a) the structure could still be modelled initially with quartic elements. Subsequently during analysis, mesh refinement into more sophisticated elements would be applied only to those quartic elements which become inaccurate due to violating the above conditions or due to material plasticity (Izzuddin *et al.*, 1995).

Kinematic and Thermal Variables

In the local Eulerian system, the quartic formulation employs eight degrees of freedom, as shown in Fig. 2, with eight corresponding element forces:

$${}^c\mathbf{u} = \langle \theta_{1y}, \theta_{2y}, \delta_{my}, \theta_{1z}, \theta_{2z}, \delta_{mz}, \theta_T, \Delta \rangle^T \quad (2.a)$$

$$c^f = \langle M_{1y}, M_{2y}, F_{my}, M_{1z}, M_{2z}, F_{mz}, M_T, F \rangle^T \quad (2.b)$$

Transverse imperfections of the centroidal reference line are defined in terms of six variables associated with the first six local degrees of freedom, whereas twist and axial imperfections are ignored:

$$c^i u = \langle \theta_{1y}^i, \theta_{2y}^i, \delta_{my}^i, \theta_{1z}^i, \theta_{2z}^i, \delta_{mz}^i, 0, 0 \rangle^T \quad (3)$$

Quartic shape functions can therefore be employed for the interpolation of transverse displacements and imperfections (v, w, v^i, w^i) , whereas a linear shape function can be used for the interpolation of the twist rotation (α) . No shape function is required herein for the axial displacement (u) , since the constant axial force criterion will be employed, as discussed in the following section.

$$v(x) = (2L \{\theta_{2y} - \theta_{1y}\} + 16\delta_{my}) \left(\frac{x}{L}\right)^4 + (L \{\theta_{2y} + \theta_{1y}\}) \left(\frac{x}{L}\right)^3 - \left(\frac{L}{2} \{\theta_{2y} - \theta_{1y}\} + 8\delta_{my}\right) \left(\frac{x}{L}\right)^2 - \left(\frac{L}{4} \{\theta_{2y} + \theta_{1y}\}\right) \left(\frac{x}{L}\right) + \delta_{my} \quad (4.a)$$

$$w(x) = (2L \{\theta_{2z} - \theta_{1z}\} + 16\delta_{mz}) \left(\frac{x}{L}\right)^4 + (L \{\theta_{2z} + \theta_{1z}\}) \left(\frac{x}{L}\right)^3 - \left(\frac{L}{2} \{\theta_{2z} - \theta_{1z}\} + 8\delta_{mz}\right) \left(\frac{x}{L}\right)^2 - \left(\frac{L}{4} \{\theta_{2z} + \theta_{1z}\}\right) \left(\frac{x}{L}\right) + \delta_{mz} \quad (4.b)$$

$$v^i(x) = (2L \{\theta_{2y}^i - \theta_{1y}^i\} + 16\delta_{my}^i) \left(\frac{x}{L}\right)^4 + (L \{\theta_{2y}^i + \theta_{1y}^i\}) \left(\frac{x}{L}\right)^3 - \left(\frac{L}{2} \{\theta_{2y}^i - \theta_{1y}^i\} + 8\delta_{my}^i\right) \left(\frac{x}{L}\right)^2 - \left(\frac{L}{4} \{\theta_{2y}^i + \theta_{1y}^i\}\right) \left(\frac{x}{L}\right) + \delta_{my}^i \quad (4.c)$$

$$w^i(x) = (2L \{\theta_{2z}^i - \theta_{1z}^i\} + 16\delta_{mz}^i) \left(\frac{x}{L}\right)^4 + (L \{\theta_{2z}^i + \theta_{1z}^i\}) \left(\frac{x}{L}\right)^3 - \left(\frac{L}{2} \{\theta_{2z}^i - \theta_{1z}^i\} + 8\delta_{mz}^i\right) \left(\frac{x}{L}\right)^2 - \left(\frac{L}{4} \{\theta_{2z}^i + \theta_{1z}^i\}\right) \left(\frac{x}{L}\right) + \delta_{mz}^i \quad (4.d)$$

$$\alpha(x) = \frac{\theta_T}{2} + \theta_T \left(\frac{x}{L}\right) \quad (4.e)$$

With the assumption of small local displacements, the generalised strains can be obtained from the following expressions:

$$\varepsilon_c = \frac{du}{dx} + \frac{1}{2} \left(\left\{ \frac{dv}{dx} + \frac{dv^i}{dx} \right\}^2 - \left\{ \frac{dv^i}{dx} \right\}^2 + \left\{ \frac{dw}{dx} + \frac{dw^i}{dx} \right\}^2 - \left\{ \frac{dw^i}{dx} \right\}^2 \right) \quad (5.a)$$

$$\kappa_y = \frac{d^2v}{dx^2} \quad (5.b)$$

$$\kappa_z = \frac{d^2w}{dx^2} \quad (5.c)$$

$$\xi = \frac{d\alpha}{dx} \quad (5.d)$$

Note that the expression for the centroidal axial strain (ε_c) accounts for stretching due to bending, which is responsible for the ability of the quartic formulation to represent the beam-column effect.

The variation of temperature over the cross-section is represented by three variables (t_c, t'_y, t'_z), corresponding to a centroidal value and rates of change in the local y and z directions, respectively. In the context of elastic analysis, these variables would be sufficient to represent any distribution of temperatures over the cross-section, including linear variation, as shown in Appendix A.1. The quartic element employs discrete temperature variables ${}_c t$ at the two end nodes and at mid-length, allowing parabolic functions to be used for the interpolation of these variables along the element length, as given below:

$${}_c t = \langle t_{1c}, t_{2c}, t_{mc}, t'_{1y}, t'_{2y}, t'_{my}, t'_{1z}, t'_{2z}, t'_{mz} \rangle^T \quad (6)$$

$$t_c(x) = t_{mc} + (t_{2c} - t_{1c}) \left(\frac{x}{L} \right) + (2 \{ t_{1c} + t_{2c} - 2t_{mc} \}) \left(\frac{x}{L} \right)^2 \quad (7.a)$$

$$t'_y(x) = t'_{my} + (t'_{2y} - t'_{1y}) \left(\frac{x}{L} \right) + (2 \{ t'_{1y} + t'_{2y} - 2t'_{my} \}) \left(\frac{x}{L} \right)^2 \quad (7.b)$$

$$t'_z(x) = t'_{mz} + (t'_{2z} - t'_{1z}) \left(\frac{x}{L} \right) + (2 \{ t'_{1z} + t'_{2z} - 2t'_{mz} \}) \left(\frac{x}{L} \right)^2 \quad (7.c)$$

The thermal generalised strains ($\varepsilon_c^t, \kappa_y^t, \kappa_z^t$), required in (1) for the determination of the cross-sectional generalised stresses, are related to the temperature variables by the coefficient of thermal expansion (γ), which is assumed herein to be constant:

$$\varepsilon_c^t = \gamma t_c \quad (8.a)$$

$$\kappa_y^t = -\gamma t'_y \quad (8.b)$$

$$\kappa_z^t = -\gamma t'_z \quad (8.c)$$

Given a set of local element displacements ${}_c u$ and temperature values ${}_c t$, kinematic and thermal generalised strains at any longitudinal position (x) can be established from (4)-(5) and (7)-(8), respectively, and the cross-sectional generalised stresses can thereafter be determined from (1).

Local Forces

In the determination of the local element forces ${}_c f$, the variation of the elastic moduli (E) and (G) along the element length is accounted for by using quadratic expressions which interpolate discrete values at the two end nodes and at mid-length:

$$E(x) = E_m + (E_2 - E_1)\left(\frac{x}{L}\right) + (2\{E_1 + E_2 - 2E_m\})\left(\frac{x}{L}\right)^2 \quad (9.a)$$

$$G(x) = G_m + (G_2 - G_1)\left(\frac{x}{L}\right) + (2\{G_1 + G_2 - 2G_m\})\left(\frac{x}{L}\right)^2 \quad (9.b)$$

The element axial force is obtained through the combination of (1.a) and (5.a) into the following expression:

$$f = EA \left[\frac{du}{dx} + \frac{1}{2} \left(\left\{ \frac{dv}{dx} + \frac{dv^i}{dx} \right\}^2 - \left\{ \frac{dv^i}{dx} \right\}^2 + \left\{ \frac{dw}{dx} + \frac{dw^i}{dx} \right\}^2 - \left\{ \frac{dw^i}{dx} \right\}^2 \right) - \varepsilon_c^t \right] \quad (10)$$

With a linear shape function for the axial displacement (u), the axial force (f) would not be constant along the element, and thus axial equilibrium would be violated. The approach followed herein is to use the constant axial force criterion, which imposes axial equilibrium instead of a shape function for the axial displacement (u):

$$f = F = \text{constant} \Rightarrow$$

$$\begin{aligned}
\int_{-L/2}^{L/2} \frac{F}{E A} dx &= \int_{-L/2}^{L/2} \left[\frac{du}{dx} + \frac{1}{2} \left(\left\{ \frac{dv}{dx} + \frac{dv^i}{dx} \right\}^2 - \left\{ \frac{dv^i}{dx} \right\}^2 + \left\{ \frac{dw}{dx} + \frac{dw^i}{dx} \right\}^2 - \left\{ \frac{dw^i}{dx} \right\}^2 \right) - \varepsilon_c^t \right] dx \Rightarrow \\
F \int_{-L/2}^{L/2} \frac{1}{E A} dx &= \Delta + \int_{-L/2}^{L/2} \left[\frac{1}{2} \left(\left\{ \frac{dv}{dx} + \frac{dv^i}{dx} \right\}^2 - \left\{ \frac{dv^i}{dx} \right\}^2 + \left\{ \frac{dw}{dx} + \frac{dw^i}{dx} \right\}^2 - \left\{ \frac{dw^i}{dx} \right\}^2 \right) - \varepsilon_c^t \right] dx \quad (11)
\end{aligned}$$

Accounting for the variation of the transverse displacements and imperfections in (4), the thermal centroidal strain given by (7.a) and (8.a), and the elastic modulus in (9.a), the integration of (11) leads to the following expression for the element axial force:

$$\begin{aligned}
F = E_f A \left[\frac{\Delta}{L} + \frac{1}{210} \left\{ 8 \left(\theta_{1y}^a{}^2 + \theta_{2y}^a{}^2 + \theta_{1z}^a{}^2 + \theta_{2z}^a{}^2 \right) + 512 \left[\left[\frac{\delta_{my}^a}{L} \right]^2 + \left[\frac{\delta_{mz}^a}{L} \right]^2 \right] \right. \right. \\
+ 5 \left(\theta_{1y}^a \theta_{2y}^a + \theta_{1z}^a \theta_{2z}^a \right) + 16 \left[\left\{ \theta_{2y}^a - \theta_{1y}^a \right\} \left[\frac{\delta_{my}^a}{L} \right] + \left\{ \theta_{2z}^a - \theta_{1z}^a \right\} \left[\frac{\delta_{mz}^a}{L} \right] \right] \\
- 8 \left(\theta_{1y}^i{}^2 + \theta_{2y}^i{}^2 + \theta_{1z}^i{}^2 + \theta_{2z}^i{}^2 \right) - 512 \left[\left[\frac{\delta_{my}^i}{L} \right]^2 + \left[\frac{\delta_{mz}^i}{L} \right]^2 \right] \\
\left. \left. - 5 \left(\theta_{1y}^i \theta_{2y}^i + \theta_{1z}^i \theta_{2z}^i \right) - 16 \left[\left\{ \theta_{2y}^i - \theta_{1y}^i \right\} \left[\frac{\delta_{my}^i}{L} \right] + \left\{ \theta_{2z}^i - \theta_{1z}^i \right\} \left[\frac{\delta_{mz}^i}{L} \right] \right] \right\} \right. \\
\left. - \frac{\gamma}{6} \{ t_{1c} + 4t_{mc} + t_{2c} \} \right] \quad (12)
\end{aligned}$$

in which,

$${}^a \mathbf{u}_c = \langle \theta_{1y}^a, \theta_{2y}^a, \delta_{my}^a, \theta_{1z}^a, \theta_{2z}^a, \delta_{mz}^a, \theta_T^a, \Delta^a \rangle^T = {}_c \mathbf{u} + {}_c^i \mathbf{u} \quad (13)$$

and,

$$E_f = \frac{L}{\int_{-L/2}^{L/2} \frac{1}{E} dx} \quad (14)$$

The above expression for (F) includes the effects of stretching due to bending, imperfections and temperature variation along the element length. Explicit expressions for (E_f) , which is an equivalent elastic modulus accounting for the variation of (E) along the length due to temperature variation, are given in Appendix A.2 in terms of the three discrete values (E_1, E_2, E_m) .

The remaining components of the local force vector ${}_c f$ are obtained using the virtual work method:

$${}_c f_i = \int_{-\frac{L}{2}}^{\frac{L}{2}} \left(f \frac{\partial \varepsilon_c}{\partial u_i} + m_y \frac{\partial \kappa_y}{\partial u_i} + m_z \frac{\partial \kappa_z}{\partial u_i} + m_T \frac{\partial \xi}{\partial u_i} \right) dx \quad \text{for } i = 1, 7 \quad (15)$$

Noting that (f) is constant along the element length, and accounting for the generalised stresses and strains derived previously in terms of the element local displacements and temperature variables, the integration of (15) leads to the following explicit expression for the local element forces:

$${}_c f = {}_u k \quad {}_c u + {}_f k \quad {}_c u + {}_t k \quad {}_c t + {}_f f \quad (16)$$

in which,

$${}_u k = \begin{bmatrix} \begin{matrix} \text{y}^k & \begin{matrix} \text{---} & \text{---} & \text{---} \\ 3 \times 3 & 0 & 3 \times 1 & 0 \end{matrix} & \begin{matrix} \text{---} & \text{---} \\ 3 \times 1 & 0 \end{matrix} & \begin{matrix} \text{---} & \text{---} \\ 3 \times 1 & 0 \end{matrix} \end{matrix} \\ \begin{matrix} \text{z}^k & \begin{matrix} \text{---} & \text{---} & \text{---} \\ 3 \times 3 & 0 & 3 \times 1 & 0 \end{matrix} & \begin{matrix} \text{---} & \text{---} \\ 3 \times 1 & 0 \end{matrix} & \begin{matrix} \text{---} & \text{---} \\ 3 \times 1 & 0 \end{matrix} \end{matrix} \\ \begin{matrix} \text{T}^k & \begin{matrix} \text{---} & \text{---} & \text{---} \\ 1 \times 3 & 0 & 1 \times 3 & 0 \end{matrix} & \begin{matrix} \text{---} & \text{---} \\ 1 \times 1 & 0 \end{matrix} & \begin{matrix} \text{---} & \text{---} \\ 1 \times 1 & 0 \end{matrix} \end{matrix} \\ \begin{matrix} \text{u}^k & \begin{matrix} \text{---} & \text{---} & \text{---} \\ 1 \times 3 & 0 & 1 \times 3 & 0 \end{matrix} & \begin{matrix} \text{---} & \text{---} \\ 1 \times 1 & 0 \end{matrix} & \begin{matrix} \text{---} & \text{---} \\ 1 \times 1 & 0 \end{matrix} \end{matrix} \end{bmatrix} \quad (17.a)$$

$${}_y k = I_y \begin{bmatrix} \begin{matrix} \frac{7.2}{L} E_{1,1} & \frac{-1.2}{L} E_{1,2} & \frac{-25.6}{L^2} E_{1,3} \end{matrix} \\ \begin{matrix} \frac{-1.2}{L} E_{2,1} & \frac{7.2}{L} E_{2,2} & \frac{25.6}{L^2} E_{2,3} \end{matrix} \\ \begin{matrix} \frac{-25.6}{L^2} E_{3,1} & \frac{25.6}{L^2} E_{3,2} & \frac{204.8}{L^3} E_{3,3} \end{matrix} \end{bmatrix} \quad (17.b)$$

$$z_k = I_z \begin{bmatrix} \frac{7.2}{L} E_{1,1} & -\frac{1.2}{L} E_{1,2} & -\frac{25.6}{L^2} E_{1,3} \\ -\frac{1.2}{L} E_{2,1} & \frac{7.2}{L} E_{2,2} & \frac{25.6}{L^2} E_{2,3} \\ -\frac{25.6}{L^2} E_{3,1} & \frac{25.6}{L^2} E_{3,2} & \frac{204.8}{L^3} E_{3,3} \end{bmatrix} \quad (17.c)$$

$$T_{uk} = \begin{bmatrix} G_e J \\ L \end{bmatrix} \quad (17.d)$$

$$f_k = \begin{bmatrix} \begin{matrix} y_k \\ f_k \end{matrix} \begin{matrix} \left| \begin{matrix} 3 \times 3 \\ 0 \end{matrix} \right| \begin{matrix} \left| \begin{matrix} 3 \times 2 \\ 0 \end{matrix} \right| \end{matrix} \\ \begin{matrix} 3 \times 3 \\ 0 \end{matrix} \begin{matrix} \left| \begin{matrix} z_k \\ f_k \end{matrix} \right| \begin{matrix} \left| \begin{matrix} 3 \times 2 \\ 0 \end{matrix} \right| \end{matrix} \\ \begin{matrix} 2 \times 3 \\ 0 \end{matrix} \begin{matrix} \left| \begin{matrix} 2 \times 3 \\ 0 \end{matrix} \right| \begin{matrix} \left| \begin{matrix} 2 \times 2 \\ 0 \end{matrix} \right| \end{matrix} \end{bmatrix} \quad (18.a)$$

$$y_k = z_k = \begin{bmatrix} \frac{8FL}{105} & \frac{FL}{42} & -\frac{8F}{105} \\ \frac{FL}{42} & \frac{8FL}{105} & \frac{8F}{105} \\ -\frac{8F}{105} & \frac{8F}{105} & \frac{512F}{105L} \end{bmatrix} \quad (18.b)$$

$$t_k = \begin{bmatrix} \begin{matrix} 3 \times 3 \\ 0 \end{matrix} \begin{matrix} \left| \begin{matrix} y_k \\ t_k \end{matrix} \right| \begin{matrix} \left| \begin{matrix} 3 \times 3 \\ 0 \end{matrix} \right| \end{matrix} \\ \begin{matrix} 3 \times 3 \\ 0 \end{matrix} \begin{matrix} \left| \begin{matrix} z_k \\ t_k \end{matrix} \right| \begin{matrix} \left| \begin{matrix} 2 \times 3 \\ 0 \end{matrix} \right| \end{matrix} \\ \begin{matrix} 2 \times 3 \\ 0 \end{matrix} \begin{matrix} \left| \begin{matrix} 2 \times 3 \\ 0 \end{matrix} \right| \begin{matrix} \left| \begin{matrix} 2 \times 3 \\ 0 \end{matrix} \right| \end{matrix} \end{bmatrix} \quad (19.a)$$

$$y_k = \gamma I_y \begin{bmatrix} -\frac{14}{15} t_{E_{1,1}} & \frac{1}{15} t_{E_{1,2}} & -\frac{2}{15} t_{E_{1,3}} \\ -\frac{1}{15} t_{E_{2,1}} & \frac{14}{15} t_{E_{2,2}} & \frac{2}{15} t_{E_{2,3}} \\ \frac{32}{15L} t_{E_{3,1}} & \frac{32}{15L} t_{E_{3,2}} & -\frac{64}{15L} t_{E_{3,2}} \end{bmatrix} \quad (19.b)$$

$$z_k = \gamma I_z \begin{bmatrix} -\frac{14}{15} t_{E_{1,1}} & \frac{1}{15} t_{E_{1,2}} & -\frac{2}{15} t_{E_{1,3}} \\ -\frac{1}{15} t_{E_{2,1}} & \frac{14}{15} t_{E_{2,2}} & \frac{2}{15} t_{E_{2,3}} \\ \frac{32}{15L} t_{E_{3,1}} & \frac{32}{15L} t_{E_{3,2}} & -\frac{64}{15L} t_{E_{3,2}} \end{bmatrix} \quad (19.c)$$

$$f_k = \langle 0, 0, 0, 0, 0, 0, 0, F \rangle^T \quad (20)$$

where,

${}_{m \times n}0$:	(m×n) zero matrix
$E \& \iota E$:	(3×3) matrices of equivalent elastic moduli
G_e :	Equivalent shear modulus
F :	Element axial force given by (12).

The first term in (16) ${}_{u}k {}_{c}u$ represents the linear bending and torsional response of the quartic element, whereas the second term ${}_{f}k {}_{c}u$ models the influence of the axial force on the bending moments, that is the beam-column effect. The temperature effects on the bending moments are modelled by the term ${}_{t}k {}_{c}t$, whereas ${}_{f}f$ is merely a vector storing the value of (F) as obtained from (12). The equivalent elastic moduli, E and ιE , account for the variation of (E) along the length due to temperature variation and are given explicitly in Appendix A.3 along with the expression for G_e .

In the context of the adopted Eulerian approach (Izzuddin & Elnashai, 1993-b), only the terms of ${}_{c}u$ associated with the end freedoms are related to the global nodal displacements, and hence the internal element displacements $(\delta_{my}, \delta_{mz})$ should be determined through a process of static condensation. If the equivalent element loads corresponding to the midside freedoms are (P_{my}, P_{mz}) , then the internal element displacements can be found through an iterative procedure as follows:

1. Initialise $(\delta_{my}, \delta_{mz})$ to values obtained in the last equilibrium step
2. Obtain the corresponding local forces (F_{my}, F_{mz}) from the appropriate terms of ${}_{c}f$ in (16)
3. Determine the iterative increment of $(\delta_{my}, \delta_{mz})$:

$$\begin{Bmatrix} \bar{\delta}_{my} \\ \bar{\delta}_{mz} \end{Bmatrix} = \begin{bmatrix} {}_{c}k_{3,3} & {}_{c}k_{3,6} \\ {}_{c}k_{6,3} & {}_{c}k_{6,6} \end{bmatrix}^{-1} \begin{Bmatrix} P_{my} - F_{my} \\ P_{mz} - F_{mz} \end{Bmatrix} \quad (20)$$

4. Update the values of $(\delta_{my}, \delta_{mz})$ by adding $(\bar{\delta}_{my}, \bar{\delta}_{mz})$
5. Repeat from (2) until $(\bar{\delta}_{my}, \bar{\delta}_{mz})$ becomes within a specified tolerance.

The ${}^b_c k$ matrix used in (20) is an (8×8) local tangent stiffness matrix derived in the following section. The equivalent midside loads (P_{my}, P_{mz}) would be zero if no internal element loads are applied, but otherwise should be determined as discussed in a later section.

Local Tangent Stiffness

The solution of the nonlinear system of equilibrium equations requires a global tangent stiffness matrix to guide the iterative procedure. A local tangent stiffness matrix ${}_c k$ is derived herein, which can be transformed into a global tangent stiffness matrix in accordance with the Eulerian approach. Before static condensation of the midside freedoms, an (8×8) local tangent stiffness matrix ${}^b_c k$ is obtained:

$${}^b_c k_{i,j} = \frac{\partial {}_c f_i}{\partial {}_c u_j} \quad \text{for } i = 1,8 \ \& \ j = 1,8 \quad (21)$$

Considering (16) and that (F) depends on the local displacements ${}_c u$ as given in (12), the following expression can be derived for ${}^b_c k$:

$${}^b_c k = {}_u k + {}_f k + E_f A L V V^T \quad (22)$$

where,

${}_u k$: (8×8) matrix given by (17)

${}_f k$: (8×8) matrix given by (18)

E_f : Equivalent elastic modulus given by (14)

and,

$$\mathbf{V} = \begin{Bmatrix} \frac{8\theta_{1y}^a}{105} + \frac{\theta_{2y}^a}{42} - \frac{8\delta_{my}^a}{105L} \\ \frac{\theta_{1y}^a}{42} + \frac{8\theta_{2y}^a}{105} + \frac{8\delta_{my}^a}{105L} \\ -\frac{8\theta_{1y}^a}{105L} + \frac{8\theta_{2y}^a}{105L} + \frac{512\delta_{my}^a}{105L^2} \\ \frac{8\theta_{1z}^a}{105} + \frac{\theta_{2z}^a}{42} - \frac{8\delta_{mz}^a}{105L} \\ \frac{\theta_{1z}^a}{42} + \frac{8\theta_{2z}^a}{105} + \frac{8\delta_{mz}^a}{105L} \\ -\frac{8\theta_{1z}^a}{105L} + \frac{8\theta_{2z}^a}{105L} + \frac{512\delta_{mz}^a}{105L^2} \\ 0 \\ \frac{1}{L} \end{Bmatrix} \quad (23)$$

The adopted Eulerian approach (Izzuddin & Elnashai, 1993-b) requires a (6×6) local tangent stiffness matrix ${}^c\mathbf{k}$ which does not include the two midside freedoms. Since the two midside forces are assumed constant within an incremental step, as discussed in the following section, ${}^c\mathbf{k}$ can be determined from ${}^b\mathbf{k}$ through a process of static condensation operating on the two midside freedoms, as given by the following expression:

$${}^c\mathbf{k}_{i,j} = {}^b\mathbf{k}_{q_i, q_j} - \frac{\mathbf{B}_{i,j}}{\mathbf{D}} \quad (24.a)$$

where,

$$\mathbf{B}_{i,j} = {}^b\mathbf{k}_{q_i,3} \left({}^b\mathbf{k}_{6,6} \quad {}^b\mathbf{k}_{3,q_j} - {}^b\mathbf{k}_{6,3} \quad {}^b\mathbf{k}_{6,q_j} \right) + {}^b\mathbf{k}_{q_i,6} \left({}^b\mathbf{k}_{3,3} \quad {}^b\mathbf{k}_{6,q_j} - {}^b\mathbf{k}_{3,6} \quad {}^b\mathbf{k}_{3,q_j} \right) \quad (24.b)$$

$$\mathbf{D} = {}^b\mathbf{k}_{3,3} \quad {}^b\mathbf{k}_{6,6} - {}^b\mathbf{k}_{3,6} \quad {}^b\mathbf{k}_{6,3} \quad (24.c)$$

$$\mathbf{q} = \{1, 2, 4, 5, 7, 8\}^T \quad (24.d)$$

Note that vector \mathbf{q} is used to store the numbers of only those local freedoms appearing in ${}^c\mathbf{u}$ which are associated with the element ends.

GLOBAL ANALYSIS

Modelling of Distributed Loads

Considering a vector W which represents distributed element loads in the three global directions, the equivalent nodal loads in the local system ${}_c p$ can be determined from W as follows:

$$W = \langle W_X, W_Y, W_Z \rangle^T \quad (25)$$

$${}_c p_i = \int_{-\frac{L}{2}}^{\frac{L}{2}} \left(W_X \frac{\partial U_X}{\partial {}_c u_i} + W_Y \frac{\partial U_Y}{\partial {}_c u_i} + W_Z \frac{\partial U_Z}{\partial {}_c u_i} \right) dx \quad (26)$$

where, U_X, U_Y and U_Z are global displacements along the element length.

In the context of an Eulerian approach, the derivatives of global element displacements, U_X, U_Y and U_Z , with respect to local freedoms ${}_c u$ depend on the current orientation of the element. Therefore, the equivalent local nodal loads ${}_c p$ vary during an incremental step, and hence such variation must be reflected within the global tangent stiffness matrix used in the nonlinear iterative procedure.

In order to avoid the above complexities, the equivalent nodal loads are obtained in a local system which is fixed during an incremental step and which coincides with the last equilibrium configuration of the element, as shown in Fig. 3. The choice of such a system is mirrored in conventional Updated Lagrangian approaches (Wen and Rahimzadeh, 1983), which assume small incremental displacements between the last equilibrium configuration and the current unknown configuration. With this assumption, the deflected shape of the quartic element can be expressed in terms of 14 local freedoms ${}_u u$ including the two midside freedoms:

$${}_u u = \langle u_{1x}, u_{1y}, u_{1z}, \alpha_{1x}, \alpha_{1y}, \alpha_{1z}, u_{2x}, u_{2y}, u_{2z}, \alpha_{2x}, \alpha_{2y}, \alpha_{2z}, \delta_{my}, \delta_{mz} \rangle^T \quad (27)$$

$$u_x(x) = \frac{1}{2}(u_{1x} + u_{2x}) + (u_{2x} - u_{1x})\left(\frac{x}{L}\right) \quad (28.a)$$

$$\begin{aligned}
u_y(x) = & \left(2L \{\alpha_{2z} - \alpha_{1z}\} + 16\delta_{my}\right) \left(\frac{x}{L}\right)^4 - \left(2 \{u_{2y} - u_{1y}\} - L \{\alpha_{1z} + \alpha_{2z}\}\right) \left(\frac{x}{L}\right)^3 \\
& - \left(\frac{L}{2} \{\alpha_{2z} - \alpha_{1z}\} + 8\delta_{my}\right) \left(\frac{x}{L}\right)^2 + \left(\frac{3}{2} \{u_{2y} - u_{1y}\} - \frac{L}{4} \{\alpha_{1z} + \alpha_{2z}\}\right) \left(\frac{x}{L}\right) \\
& + \left(\left\{\frac{u_{1y} + u_{2y}}{2}\right\} + \delta_{my}\right)
\end{aligned} \tag{28.b}$$

$$\begin{aligned}
u_z(x) = & \left(2L \{\alpha_{1y} - \alpha_{2y}\} + 16\delta_{mz}\right) \left(\frac{x}{L}\right)^4 - \left(2 \{u_{2z} - u_{1z}\} + L \{\alpha_{1y} + \alpha_{2y}\}\right) \left(\frac{x}{L}\right)^3 \\
& - \left(\frac{L}{2} \{\alpha_{1y} - \alpha_{2y}\} + 8\delta_{mz}\right) \left(\frac{x}{L}\right)^2 + \left(\frac{3}{2} \{u_{2z} - u_{1z}\} + \frac{L}{4} \{\alpha_{1y} + \alpha_{2y}\}\right) \left(\frac{x}{L}\right) \\
& + \left(\left\{\frac{u_{1z} + u_{2z}}{2}\right\} + \delta_{mz}\right)
\end{aligned} \tag{28.c}$$

Note that quartic shape functions are employed for the transverse global displacements (u_y, u_z) , whereas a linear shape function is used for the axial displacement (u_x) . It is also important to note that the two midside freedoms are referred to the current element chord, instead of the last known chord position, so that equivalent loads corresponding to the midside Eulerian freedoms can be obtained and used in the static condensation process discussed previously.

A vector of local distributed element loading ${}_u w$ is first defined, which is obtained from the global vector W given by (25) through applying a transformation matrix ${}_d T$ of direction cosines of the last known configuration with reference to the global system:

$${}_u w = \langle w_x, w_y, w_z \rangle^T = {}_d T W \tag{29}$$

The equivalent local nodal loads ${}_u p$ are then determined from ${}_u w$ as follows:

$${}_u p = \langle P_{1x}, P_{1y}, P_{1z}, R_{1x}, R_{1y}, R_{1z}, P_{2x}, P_{2y}, P_{2z}, R_{2x}, R_{2y}, R_{2z}, P_{my}, P_{mz} \rangle^T \tag{30.a}$$

$${}_u p_i = \int_{-\frac{L}{2}}^{\frac{L}{2}} \left(w_x \frac{\partial u_x}{\partial u_i} + w_y \frac{\partial u_y}{\partial u_i} + w_z \frac{\partial u_z}{\partial u_i} \right) dx \tag{30.b}$$

where the derivatives of local element displacements, u_x , u_y and u_z , with respect to local freedoms ${}_u u$ are constant during an incremental step and can be determined readily from (28). For uniformly

distributed loads, ${}_u w$ is constant over the element length, and hence the integration of (30.b) leads to the following explicit expression for the equivalent local nodal loads:

$${}_u \mathbf{P} = \frac{L}{2} \left\langle w_x, w_y, w_z, 0, \frac{-w_z L}{30}, \frac{w_y L}{30}, w_x, w_y, w_z, 0, \frac{w_z L}{30}, \frac{-w_y L}{30}, \frac{16w_y}{15}, \frac{16w_z}{15} \right\rangle^T \quad (31)$$

The first twelve terms of ${}_u \mathbf{P}$ associated with the end nodes $\left({}^e \mathbf{P} = \langle P_{1x}, \dots, R_{2z} \rangle^T \right)$ can be transformed into global equivalent nodal loads ${}^e \mathbf{P}$ through applying the same transformation matrix ${}_d \mathbf{T}$ used in (29):

$${}^e \mathbf{P} = {}_d \mathbf{T}^T {}_u \mathbf{P} \quad (32)$$

where, the equivalent loads ${}^e \mathbf{P}$ are subsequently treated as applied global nodal loads within the current incremental step.

The last two terms of ${}_u \mathbf{P}$ associated with the midside freedoms $\left({}^m \mathbf{P} = \langle P_{my}, P_{mz} \rangle^T \right)$ are used in the static condensation process discussed previously.

Solution Procedure

The quartic formulation can be used within an incremental approach employing an iterative strategy, such as the Newton-Raphson method, for the solution of the nonlinear equations of equilibrium. Within an incremental step, the applied nodal loads, the distributed element loads and the temperature distribution over the elements are prescribed, and hence the basic unknowns of the problem are the global nodal displacements which can be obtained from equilibrium considerations. In this context, the two main requirements of the iterative solution procedure are (1) the ability to establish global nodal forces given a set of global nodal displacements and, (2) the determination of a global tangent stiffness matrix which can be used for guiding the solution process.

Although the quartic formulation is derived in the local Eulerian system, transformations accounting for large global displacements and finite rotations can be used to determine its global response characteristics (Izzuddin & Elnashai, 1993-b). The first requirement of the iterative procedure can be met through transforming global displacements into local displacements, establishing the local forces

using (16), and then transforming the local forces into global forces. The second requirement is satisfied merely through transforming the local tangent stiffness matrix ${}_e k$ given by (22) into a global tangent stiffness matrix.

VERIFICATION

The proposed quartic formulation has been implemented in ADAPTIC v2.5.4 (Izzuddin, 1991; Izzuddin & Elnashai, 1992), which is a computer program for the adaptive nonlinear analysis of steel, reinforced concrete and composite framed structures. ADAPTIC is used herein to analyse several example problems which demonstrate the ability of the quartic formulation to represent accurately the response of imperfect beam-columns subject to thermal effects with only one element per member. In all examples, temperatures are incremental from a base value at which the unloaded structure under consideration is stress free.

Column

The column shown in Fig. 4.a is subjected to an eccentric axial load (P) with the pre- and post-buckling responses obtained using four different models: one quartic element based on the proposed formulation (**Q1**), one quartic element based on the formulation by So and Chan (1991), and one and four cubic elements (**C1**, **C4**) (Izzuddin & Elnashai, 1993-a). The resulting load-deflection curves given in Fig. 5 for the axial displacement demonstrate that one quartic element predicts the buckling load (P_{c1}) almost exactly, whereas one cubic element over-estimates the buckling load by over 20%. Although the quartic element proposed by So and Chan (1991) is accurate in predicting the buckling load, it over-estimates the post-buckling response considerably as compared to the more accurate results of four cubic elements. On the other hand, the quartic element proposed herein retains the post-buckling accuracy up to considerable axial displacements. This is attributed mainly to the fact that the proposed quartic formulation employs the constant axial force criterion instead of a linear shape function for the axial displacements as adopted in the formulation of So and Chan.

The same column with parabolic imperfections of $(L/2000)$ is restrained against extension, as shown in Fig. 4.b, and is subjected to two cases of thermal loading. The two cases correspond to uniform and parabolic temperature distributions over the column length, respectively, with both cases assuming no temperature variation within the cross-section. For the parabolic case, the mid-length temperature is twice the temperature at the column ends. The variation of the mid-length transverse displacement and axial force is shown in Figs. 6.a and 6.b, respectively, where the results are obtained using one quartic element (**Q1U**, **Q1P**), one cubic element (**C1U**, **C1P**) and four cubic elements (**C4U**, **C4P**) for the two cases of uniform (**U**) and parabolic (**P**) temperature distributions. These results show that one cubic element overestimates the buckling temperatures for both temperature distributions by over 20%, whereas one quartic element provides an excellent prediction of the pre- and post-buckling response in comparison with four cubic elements. The results also demonstrate that the parabolic thermal load requires a higher mid-length temperature to initiate buckling in comparison with uniform thermal loading. However, in both cases the buckling temperatures are well below the threshold temperature ($t_s = 150^\circ\text{C}$). Above this threshold temperature the elastic modulus starts decreasing, and hence the axial force required to sustain the buckling state reduces, as shown in Fig. 6.b.

The column is now restrained against rotation at one of its ends, as shown in Fig. 4.c, and is subjected to uniform and parabolic thermal loading cases, as described for the previous column. The variation of the axial force and transverse displacement is shown in Figs. 7.a and 7.b, respectively. These results demonstrate the accuracy of one quartic element (**Q1U**, **Q1P**) in predicting the temperature at which buckling occurs and the post-buckling response for the two thermal loading cases in comparison with four cubic elements (**C4U**, **C4P**). It is also shown that one cubic element (**C1U**, **C1P**) overestimates the buckling temperature by over 50% for both temperature distributions. Consideration of Fig. 7.b shows that one quartic element overestimates the axial buckling force (P_{c2}) by 3% for both loading conditions, since the quartic shape function for the transverse displacements is a slightly inaccurate representation of the associated buckling mode. Nevertheless, one quartic element provides a superior accuracy to that of one cubic element, which overestimates the buckling force for both loading conditions by approximately 40%.

Cantilever

The large displacement response of the cantilever shown in Fig. 8.a was considered by Kassimali and Abbasnia (1990), who employed a beam-column formulation based on stability functions. Comparison of the results for the (U) and (V) tip displacements in Fig. 9 shows that one quartic element provides almost identical results to those of Kassimali and Abbasnia, which they showed to be in excellent agreement with the exact analytical solution.

The response of the same cantilever to uniformly distributed loading, as shown in Fig. 8.b, is studied using 1, 2 and 4 quartic elements. The results for the (U) and (V) tip displacements, depicted in Fig. 10, show that one quartic element is capable of predicting accurately the response under distributed loading up to very large displacements ($U \leq 25\text{cm}$ & $V \leq 100\text{cm}$). The inaccuracies beyond this range of displacements are primarily attributed to the inability of one quartic element to represent the complex variation in the axial force over the cantilever length. In such a case, it is shown that two quartic elements provide favourable results over the full range of displacements under consideration.

Propped-Cantilever

The cantilever considered in the previous example is now propped at a 45° angle and supports a constant vertical load of (4.45 N) at its tip, as shown in Fig. 11, with a rigid connection assumed between the cantilever and the prop. The effect of applying uniform thermal loading to the prop is investigated using three models consisting of one cubic element per member (C1), ten cubic elements per member (C10) and one quartic element per member (Q1).

The variation of tip displacements (U) and (V) with temperature is shown in Fig. 12.a, where the results of the (C10) and (Q1) models compare favourably, thus demonstrating the accuracy of one quartic element. On the other hand, one cubic element (C1) is shown to overestimate the buckling temperature by over 10% and to provide a similar level of inaccuracy in predicting the post-buckling response. It is worth noting that buckling occurs at a prop temperature of 410°C , which is relatively high in comparison with the buckling temperatures of the restrained columns in the first example. This is primarily attributed to the flexibility of the cantilever which provides negligible resistance to

the prop thermal expansion, thus leading to an insignificant variation in the prop axial force prior to the buckling temperature, as shown in Fig. 12.b. At 410 °C, the elastic modulus of the prop has been reduced sufficiently for buckling to be initiated, with a further increase in temperature leading to a reduction in the prop axial buckling force, therefore causing a greater part of the vertical load to be taken by the cantilever. The deflected shapes of the propped cantilever at 410 °C and 500 °C are shown to scale in Fig. 13, which illustrates the high levels of deformation involved in this problem.

To illustrate the efficiency of the quartic formulation, the CPU time demands of the (C1), (C10) and (Q1) models are obtained as 0.65 sec, 2.61 sec and 0.72 sec, respectively. These figures show that one quartic element is only 11% more computationally demanding than one cubic element, while providing the same levels of accuracy of 10 cubic elements with computational savings of 72%.

CONCLUSIONS

This paper presents a new formulation for geometrically nonlinear analysis of imperfect beam-columns subject to thermal loading. The formulation is derived in a local Eulerian system, where quartic shape functions are used for the transverse displacements, and the constant axial force criterion is employed instead of shape functions for the axial displacement. In addition, the proposed formulation models transverse imperfections using quartic interpolation functions, and assumes parabolic distribution of temperature over the element length. Whilst the quartic formulation accounts for the effect of temperature variation within the cross-section on thermal stresses, it assumes a constant elastic modulus over the cross-section which is determined by the centroidal temperature. However, the variation of the elastic modulus along the element length due to variation in the centroidal temperature is modelled, where a parabolic interpolation function is used.

The quartic formulation has been implemented in the nonlinear analysis program ADAPTIC, which is used to verify the ability of the formulation to model the elastic thermal response of imperfect beam-columns using only one element per member. This proves to be an important requirement in the context of adaptive elasto-plastic analysis, since automatic mesh refinement need thus be applied during analysis only to those elements where material plasticity is detected.

It is demonstrated that one quartic element predicts accurately the buckling and post-buckling response of beam-columns, particularly for effective length factors greater than 0.7. For the case of a column rotationally-restrained at one end (i.e. effective length factor ≈ 0.7), one quartic element over-estimates the axial buckling force by 3%. However, such inaccuracies, although relatively small, diminish when the overall resistance of a structure is considered. This is partly because effective length factors of individual components in a structure often exceed 0.7, and partly due to the fact that the resistance of a buckled component represents a partial contribution to the overall structural resistance.

It is also shown that the quartic formulation models accurately and efficiently the effect of non-uniform temperature distribution along the beam-column length using only one element. In addition, it is noted that the formulation accounts for temperature variation over the cross-section, although the level of accuracy is slightly reduced when such variation leads to a non-uniform elastic modulus within the cross-section. Due to the complexity of including the effect of a varying cross-sectional elastic modulus in a formulation derived on the level of generalised actions, it is proposed that such a condition is considered in conjunction with the condition of material plasticity to control the application of automatic mesh refinement. In this context, one quartic element per member is retained during analysis until either condition is detected, after which the corresponding quartic element is refined into more computationally expensive elements which can model both conditions accurately.

REFERENCES

1. Al-Bermani, F.G.A. and Kitipornchai, S., 1990. "Nonlinear Analysis of Thin-Walled Structures Using Least Element/Member", *Journal of Structural Engineering*, ASCE, Vol. 116, No. 1, pp. 215-234.
2. Cooke, G.M.E., 1988. "An Introduction to the Mechanical Properties of Structural Steel at Elevated Temperatures", *Fire Safety Journal*, Vol. 13, pp. 45-54.

3. EC3, 1993. "Eurocode 3 – Design of Steel Structures: Part 1.2 Structural Fire Design", European Committee for Standardisation.
4. Izzuddin, B.A. and Elnashai, A.S., 1992. "ADAPTIC: A Program for the Adaptive Dynamic Analysis of Space Frames", User Manual, Imperial College.
5. Izzuddin, B.A. and Elnashai, A.S., 1993-a. "Adaptive Space Frame Analysis: Part II, A Distributed Plasticity Approach", Structures and Buildings Journal, Proceedings of the Institution of Civil Engineers, Vol. 99, No. 3, pp. 317-326.
6. Izzuddin, B.A. and Elnashai, A.S., 1993-b. "Eulerian Formulation for Large Displacement Analysis of Space Frames". Journal of Engineering Mechanics, ASCE, Vol. 119, No. 3, pp. 549-569.
7. Izzuddin, B.A. and Elnashai, A.S., 1994. "Buckling and Geometrically Nonlinear Analysis of Frames Using One Element/Member, by A.K.W. So & S.L. Chan", Discussion, Journal of Constructional Steel Research, Vol. 28, 1994, pp. 321-322.
8. Izzuddin, B.A., 1991. "Nonlinear Dynamic Analysis of Framed Structures", PhD Thesis, Department of Civil Engineering, Imperial College, London.
9. Izzuddin, B.A., Karayannis, C.G. and Elnashai, A.S., 1994. "Advanced Nonlinear Formulation for Reinforced Concrete Beam-Columns", Journal of Structural Engineering, ASCE, Vol. 120, No. 10, pp. 2913-2934.
10. Izzuddin, B.A., Song, L., and Elnashai, A.S., 1995. "Adaptive Analysis of Steel Frames Subject to Fire Loading", Computing in Civil and Building Engineering, (ICCCBE'95), P.J. Pahl and H. Werner (eds.), A.A. Balkema, Rotterdam, pp. 643-649.
11. Karayannis, C.G., Izzuddin, B.A. and Elnashai, A.S., 1994. "Application of Adaptive Analysis to Reinforced Concrete Frames", Journal of Structural Engineering, ASCE, Vol. 120, No. 10, pp. 2935-2957.

12. Kassimali, A. and Abbasnia, R., 1990. "Large Deformation Analysis of Elastic Space Frames", *Journal of Structural Engineering*, ASCE, Vol. 117, No. 7, pp. 2069-2087.
13. Kondoh, K., Tanaka, K. and Atluri, S.N., 1986. "An Explicit Expression for the Tangent-Stiffness of a Finitely Deformed 3-D Beam and its Use in the Analysis of Space Frames", *Computers & Structures*, Vol. 24, No. 2, pp. 253-271.
14. Oran, C. and Kassimali, A., 1976. "Large Deformation of Framed Structures Under Static and Dynamic Loads", *Computers & Structures*, Vol. 6, pp. 539-547.
15. Oran, C., 1973. "Tangent Stiffness in Space Frames", *Journal of the Structural Division*, ASCE, Vol. 99, No. ST6, pp. 987-1001.
16. So, A.K.W. and Chan, S.L., 1991. "Buckling and Geometrically Nonlinear Analysis of Frames Using One Element/Member", *Journal of Constructional Steel Research*, Vol. 20, pp. 271-289.
17. Soreide, T.H., Amdahl, J. and Rembar, H., 1987. "The Idealized Structural Unit Method on Space Tubular Frames", *Proceedings of International Conference on Steel & Aluminium Structures*, Cardiff, U.K., pp. 674-688.
18. Wen, R.K. and Rahimzadeh, J., 1983. "Nonlinear Elastic Frame Analysis by Finite Element", *Journal of Structural Engineering*, ASCE, Vol. 109, No. 8, pp. 1952-1971.

APPENDIX A

A.1. Equivalent Thermal Variables

Given a temperature distribution $t(y,z)$ over the cross-section, the generalised stresses due to thermal strains can be established as follows:

$$f^t = \int -E\gamma t \, dA \quad (33.a)$$

$$m_y^t = \int E\gamma t y \, dA \quad (33.b)$$

$$m_z^t = \int E\gamma t z \, dA \quad (33.c)$$

The values of thermal variables (t_c, t'_y, t'_z) can be established to correspond to the same values of generalised stresses associated with $t(y,z)$ and given by (33). Therefore, the following simultaneous equations must be satisfied:

$$\int -E\gamma (t_c + t'_y y + t'_z z) \, dA = f^t \quad (34.a)$$

$$\int E\gamma (t_c + t'_y y + t'_z z) y \, dA = m_y^t \quad (34.b)$$

$$\int E\gamma (t_c + t'_y y + t'_z z) z \, dA = m_z^t \quad (34.c)$$

Since the y and z axes are principal axes of bending and have their origin at the cross-section centroid, the following equalities apply:

$$\int y \, dA = \int z \, dA = \int yz \, dA = 0 \quad (35)$$

Considering (33)-(35) with the assumption that (E) and (γ) are constant over the cross-section, the following equivalent thermal variables can be established from $t(y,z)$:

$$t_c = \frac{\int t \, dA}{\int dA} = \frac{\int t \, dA}{A} \quad (36.a)$$

$$t'_y = \frac{\int t y \, dA}{\int y^2 \, dA} = \frac{\int t y \, dA}{I_y} \quad (36.b)$$

$$t'_z = \frac{\int t z \, dA}{\int z^2 \, dA} = \frac{\int t z \, dA}{I_z} \quad (36.c)$$

A.2. Elastic Modulus E_f

The equivalent elastic modulus E_f needed for axial force calculation depends on the values of the elastic modulus at the element ends and mid-length (E_1, E_2, E_m), which may be different due to temperature variation along the element length. Considering (9.a) in conjunction with (14), the following expressions for E_f can be derived:

$$E_f = E_m \quad (\text{if } E_1 = E_2 = E_m) \quad (37.a)$$

$$E_f = \frac{E_1 - E_2}{\log\left(\frac{E_1}{E_2}\right)} \quad \left(\text{if } E_m = \frac{E_1 + E_2}{2}\right) \quad (37.b)$$

$$E_f = \frac{\sqrt{\eta}}{\log\left(\frac{\{1 + \chi\}\{1 - \phi\}}{\{1 - \chi\}\{1 + \phi\}}\right)} \quad (\text{if } \eta > 0) \quad (37.c)$$

$$E_f = \frac{\sqrt{-\eta}}{2[\tan^{-1}(\phi) - \tan^{-1}(\chi)]} \quad (\text{if } \eta < 0) \quad (37.d)$$

where,

$$\eta = (4E_m - E_1 - E_2)^2 - 4E_1E_2 \quad (38.a)$$

$$\chi = \frac{(4E_m - E_1 - 3E_2)}{\sqrt{|\eta|}} \quad (38.b)$$

$$\phi = \frac{(-4E_m + 3E_1 + E_2)}{\sqrt{|\eta|}} \quad (38.c)$$

Note that if the elastic modulus (E) is uniform along the element length, then the equivalent elastic modulus E_f reduces to this constant value.

A.3. Elastic Modulii E , tE and G_e

The matrices of equivalent elastic modulii E and tE , used in (17) and (19), depend on the three discrete values for the elastic modulus (E_1, E_2, E_m), and are expressed as follows:

$$E = \begin{bmatrix} \frac{529E_1 - 17E_2 + 244E_m}{756} & \frac{67E_1 + 67E_2 - 8E_m}{126} & \frac{25E_1 + 4E_2 + 13E_m}{42} \\ \frac{67E_1 + 67E_2 - 8E_m}{126} & \frac{-17E_1 + 529E_2 + 244E_m}{756} & \frac{4E_1 + 25E_2 + 13E_m}{42} \\ \frac{25E_1 + 4E_2 + 13E_m}{42} & \frac{4E_1 + 25E_2 + 13E_m}{42} & \frac{11E_1 + 11E_2 + 20E_m}{42} \end{bmatrix} \quad (39.a)$$

$${}^tE = \begin{bmatrix} \frac{143E_1 - 11E_2 + 64E_m}{196} & \frac{11E_1 - 17E_2 + 20E_m}{14} & \frac{16E_1 - 5E_2 - 4E_m}{7} \\ \frac{-17E_1 + 11E_2 + 20E_m}{14} & \frac{-11E_1 + 143E_2 + 64E_m}{196} & \frac{-5E_1 + 16E_2 - 4E_m}{7} \\ \frac{13E_1 - E_2 + 2E_m}{14} & \frac{-E_1 + 13E_2 + 2E_m}{14} & \frac{-E_1 - E_2 + 16E_m}{14} \end{bmatrix} \quad (39.b)$$

Note that if the elastic modulus (E) is uniform along the element length, then all the terms of E and tE reduce to this constant value.

The equivalent elastic shear modulus (G_e), used in (17), can be expressed in terms of the three discrete values (G_1, G_2, G_m) as follows:

$$G_e = \frac{G_1 + G_2 + 4G_m}{6} \quad (40)$$

Note again that if the shear modulus (G) is uniform along the element length, then the equivalent shear modulus (G_e) reduces to this constant value.

APPENDIX B: NOTATION

- Generic symbols of matrices and vectors are represented by bold font-type with left side subscripts or superscripts (e.g. ${}_c\mathbf{u}$, ${}^b\mathbf{k}$).
- Subscripts and superscripts to the right side of the generic symbol indicate the term of the vector or matrix under consideration (e.g. ${}_c\mathbf{u}_i$, ${}^b\mathbf{k}_{3,3}$).

Operators

- T : right-side superscript, transpose sign.
- : incremental operator for variables (e.g. \bar{y})
- ∂ : partial differentiation.
- [] : encloses terms of a matrix.
- $\langle \rangle$: encloses terms of a row vector.
- $\{ \}$: encloses terms of a column vector.

Symbols

- A : cross-sectional area
- E : Young's elastic modulus; (E_1, E_2, E_m) represent discrete values of (E) at the two end nodes and mid-length
- E : (3×3) matrix of equivalent elastic moduli for bending stiffness
- E_f : equivalent elastic modulus for axial stiffness
- ${}_t\mathbf{E}$: (3×3) matrix of equivalent elastic moduli for thermal effects on bending
- f : axial force; generalised stress
- ${}_c\mathbf{f}$: local element forces; $\langle M_{1y}, M_{2y}, F_{my}, M_{1z}, M_{2z}, F_{mz}, M_T, F \rangle^T$

- G : elastic shear modulus; (G_1, G_2, G_m) represent discrete values of (G) at the two end nodes and mid-length
- G_e : equivalent shear modulus
- I_y : cross-sectional second moment of area in local y direction
- I_z : cross-sectional second moment of area in local z direction
- J : St. Venant's torsion constant
- ${}^c k$: (6×6) local tangent stiffness matrix after static condensation
- ${}^b k$: (8×8) local tangent stiffness matrix before static condensation
- ${}^f k$: (8×8) stiffness matrix representing beam-column effect; includes ${}^y k$ and ${}^z k$
- ${}^t k$: (8×9) matrix modelling thermal effects on bending; includes ${}^y k$ and ${}^z k$
- ${}^u k$: (8×8) linear bending stiffness matrix; includes ${}^y k$, ${}^z k$ and ${}^T k$
- L : element length
- m_y : bending moment in y-direction; generalised stress
- m_z : bending moment in z-direction; generalised stress
- m_T : torsional moment; generalised stress
- ${}^u p$: equivalent local nodal loads; includes ${}^e p$ and ${}^m p$;
 $\langle P_{1x}, P_{1y}, P_{1z}, R_{1x}, R_{1y}, R_{1z}, P_{2x}, P_{2y}, P_{2z}, R_{2x}, R_{2y}, R_{2z}, P_{my}, P_{mz} \rangle^T$
- t : temperature
- t_c : centroidal temperature; generalised strain
- ${}^c t$: vector of temperature variables; $\langle t_{1c}, t_{2c}, t_{mc}, t'_{1y}, t'_{2y}, t'_{my}, t'_{1z}, t'_{2z}, t'_{mz} \rangle^T$
- t'_y : rate of temperature change in local y direction; generalised strain
- t'_z : rate of temperature change in local z direction; generalised strain
- ${}^d T$: transformation matrix of direction cosines

- u : axial displacement
- ${}_c u$: local element freedoms; $\langle \theta_{1y}, \theta_{2y}, \delta_{my}, \theta_{1z}, \theta_{2z}, \delta_{mz}, \theta_T, \Delta \rangle^T$
- ${}_c^a u$: local element displacements including imperfections;
 $\langle \theta_{1y}^a, \theta_{2y}^a, \delta_{my}^a, \theta_{1z}^a, \theta_{2z}^a, \delta_{mz}^a, \theta_T^a, \Delta^a \rangle^T$
- ${}_c^i u$: local element imperfections; $\langle \theta_{1y}^i, \theta_{2y}^i, \delta_{my}^i, \theta_{1z}^i, \theta_{2z}^i, \delta_{mz}^i, 0, 0 \rangle^T$
- ${}_u u$: local element freedoms for equivalent nodal loads calculation;
 $\langle u_{1x}, u_{1y}, u_{1z}, \alpha_{1x}, \alpha_{1y}, \alpha_{1z}, u_{2x}, u_{2y}, u_{2z}, \alpha_{2x}, \alpha_{2y}, \alpha_{2z}, \delta_{my}, \delta_{mz} \rangle^T$
- v : transverse element displacement in local y direction
- v^i : transverse element imperfection in local y direction
- w : transverse element displacement in local z direction
- W : distributed element loads in global system; $\langle W_X, W_Y, W_Z \rangle^T$
- w^i : transverse element imperfection in local z direction
- ${}_u w$: distributed element loads in local system; $\langle w_x, w_y, w_z \rangle^T$
- α : element rotational twist
- ε_c : centroidal generalised strain
- ε_c^t : centroidal thermal strain
- γ : coefficient of thermal expansion
- κ_y : generalised curvature strain in y direction
- κ_y^t : thermal curvature strain in y direction
- κ_z : generalised curvature strain in z direction
- κ_z^t : thermal curvature strain in z direction
- ξ : rate of twist generalised strain

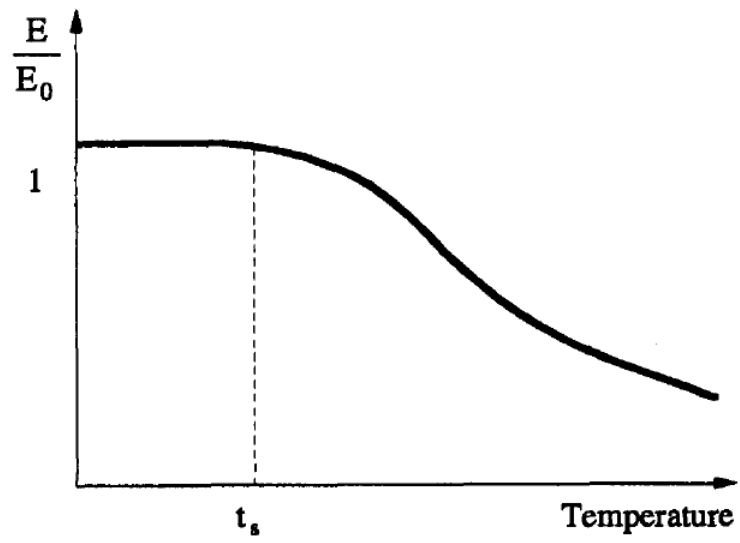


Fig. 1 Effect of temperature on elastic modulus

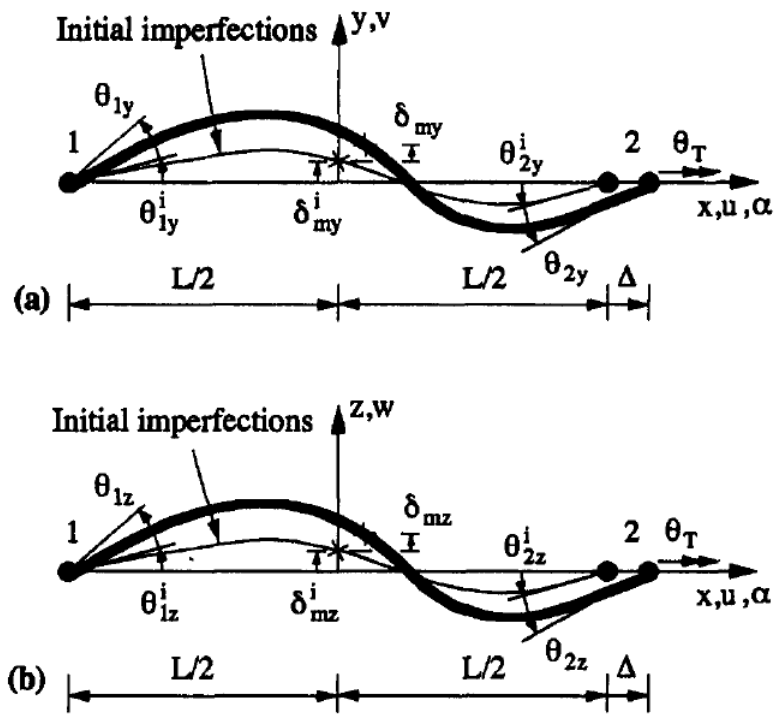


Fig. 2 Local degrees of freedom of quartic formulation

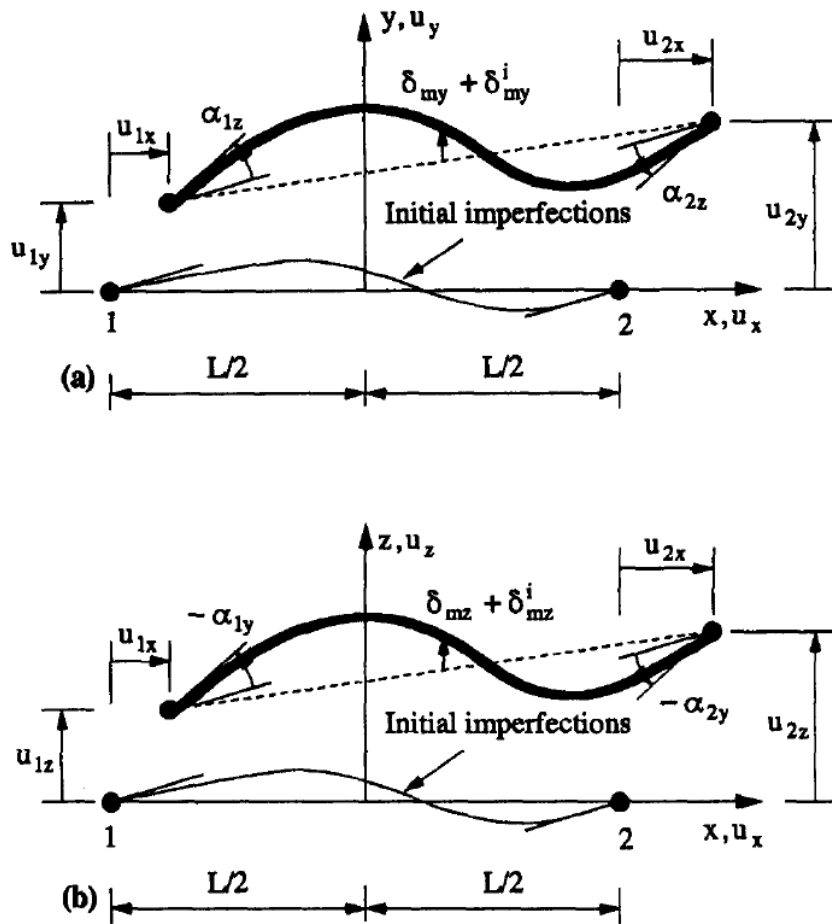
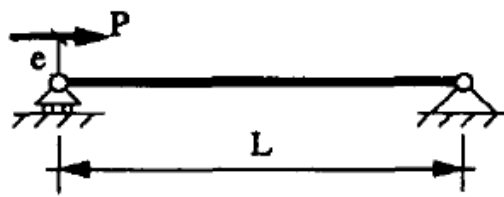
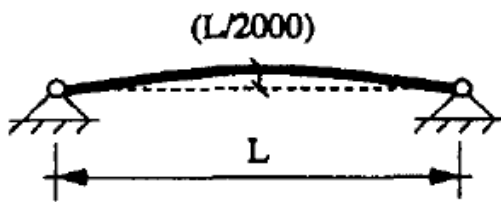


Fig. 3 Local system for equivalent nodal load calculation

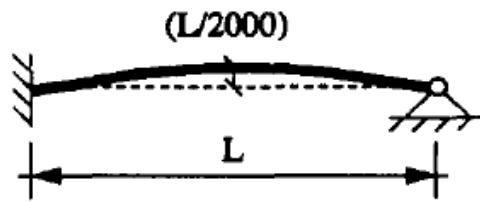


(a) Pin-ended under eccentric load

$$\begin{aligned}
 &e = 0.254 \text{ cm}, \quad L = 254 \text{ cm} \\
 &I = 34.68 \text{ cm}^4, \quad A = 6.452 \text{ cm}^2 \\
 &E = \begin{cases} 68970 \text{ MPa} & \text{for } (t \leq 150^\circ \text{C}) \\ (95580 - 177.4t) \text{ MPa} & \text{for } (150^\circ \text{C} < t \leq 500^\circ \text{C}) \end{cases} \\
 &\gamma = 2 \times 10^{-5} \text{ }^\circ \text{C}^{-1}
 \end{aligned}$$



(b) Pin-ended under thermal load



(c) Rotationally restrained at one end

Fig. 4 Column subject to three cases of boundary conditions

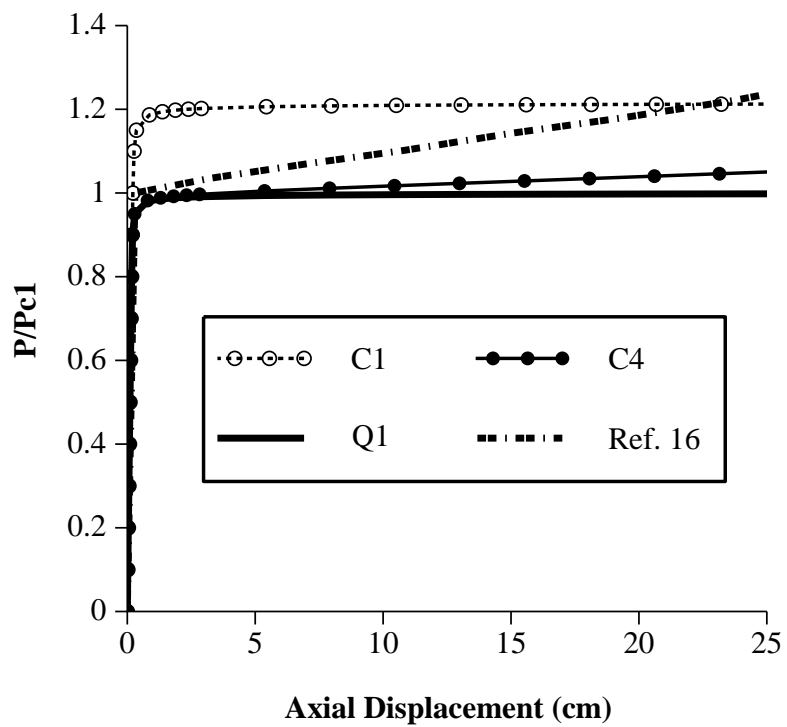


Fig. 5 Buckling of eccentrically-loaded column: axial displacement

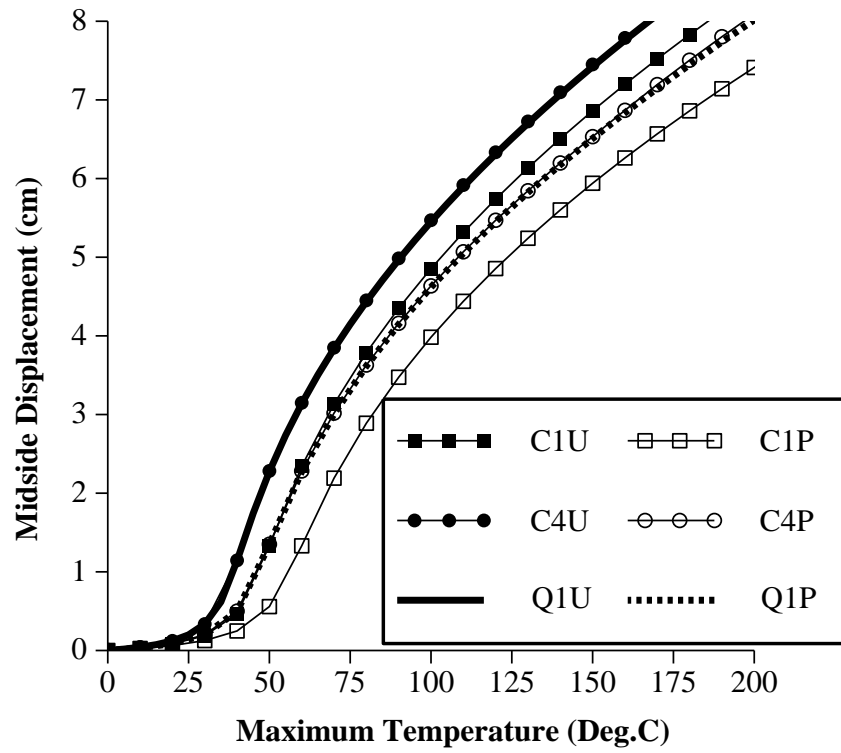


Fig. 6.a Thermal buckling of pin-ended column: transverse displacement

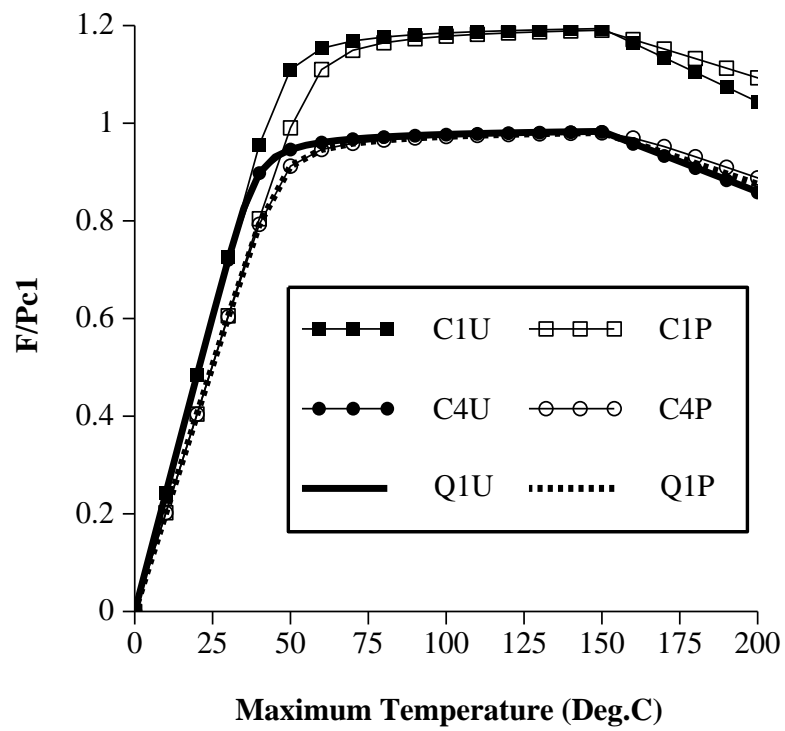


Fig. 6.b Thermal buckling of pin-ended column: axial force

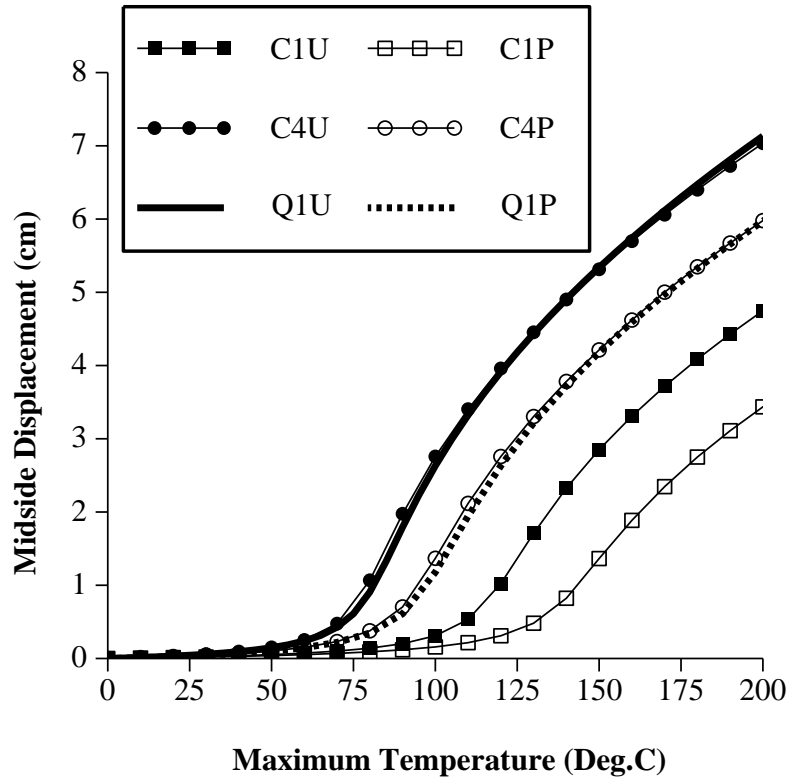


Fig. 7.a Thermal buckling of rotationally-restrained column: transverse displacement

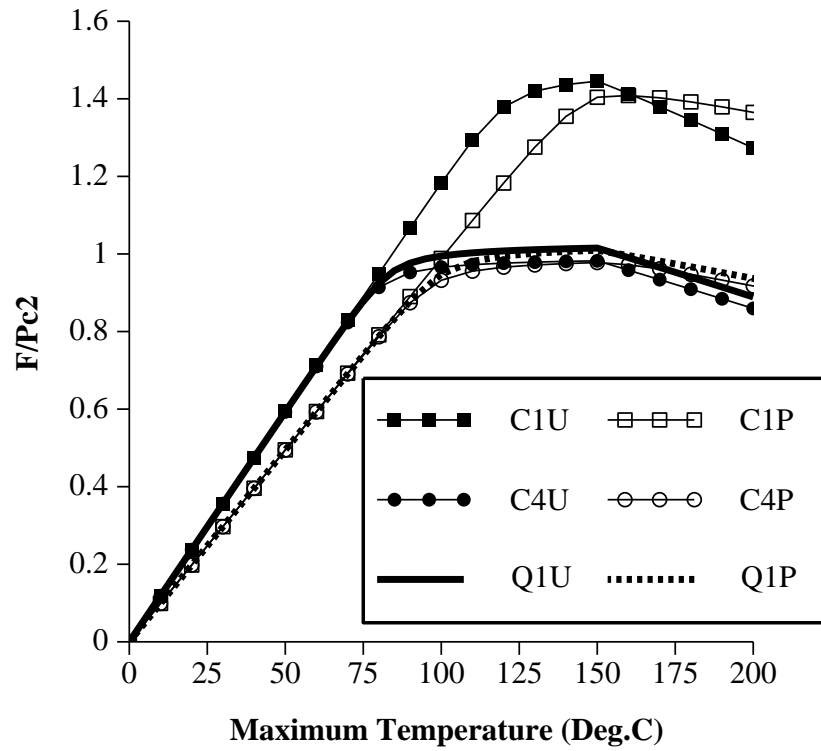


Fig. 7.b Thermal buckling of rotationally-restrained column: axial force

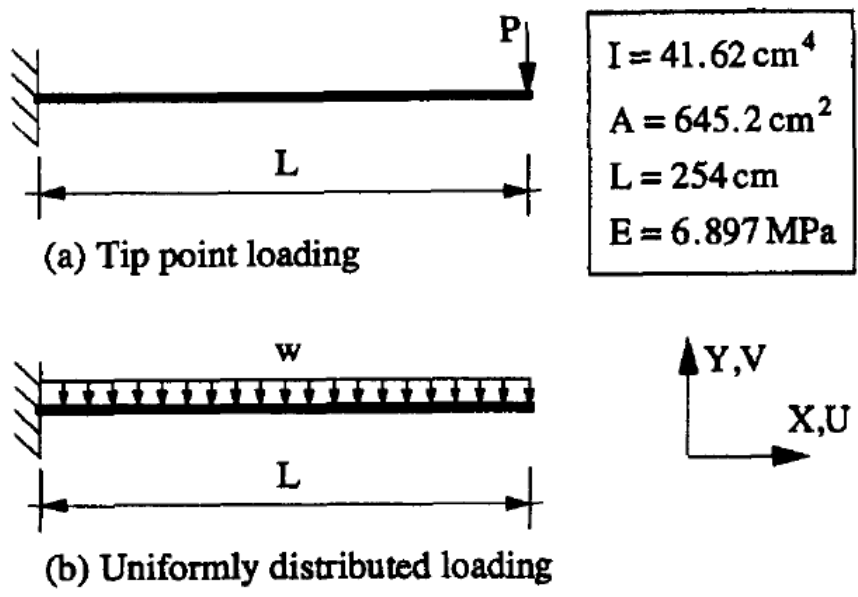


Fig. 8 Cantilever subject to two loading cases

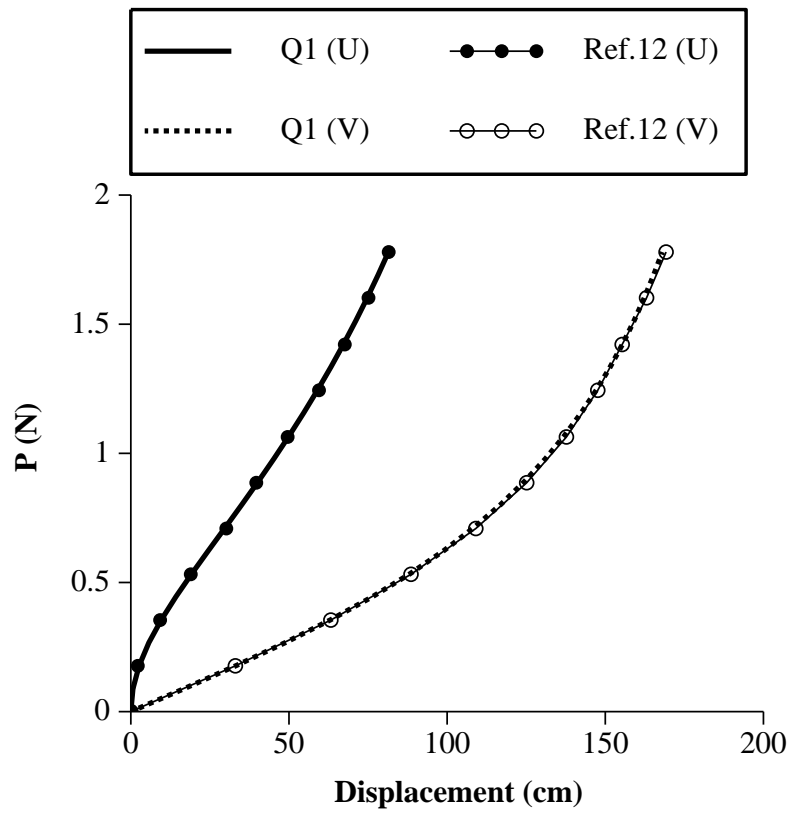


Fig. 9 Response of cantilever to point loading

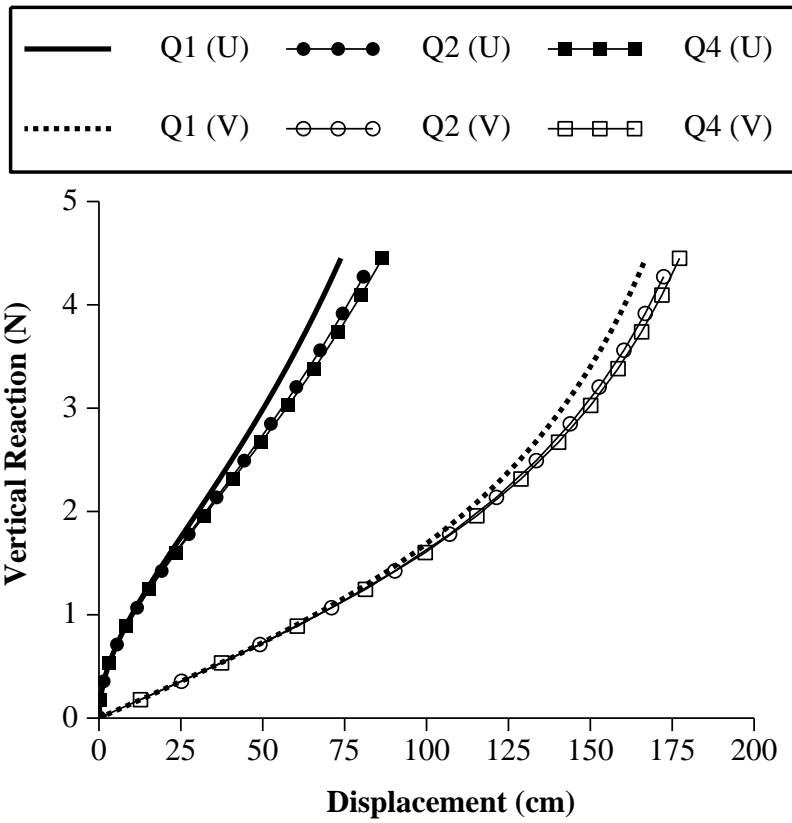


Fig. 10 Response of cantilever to uniformly distributed loading

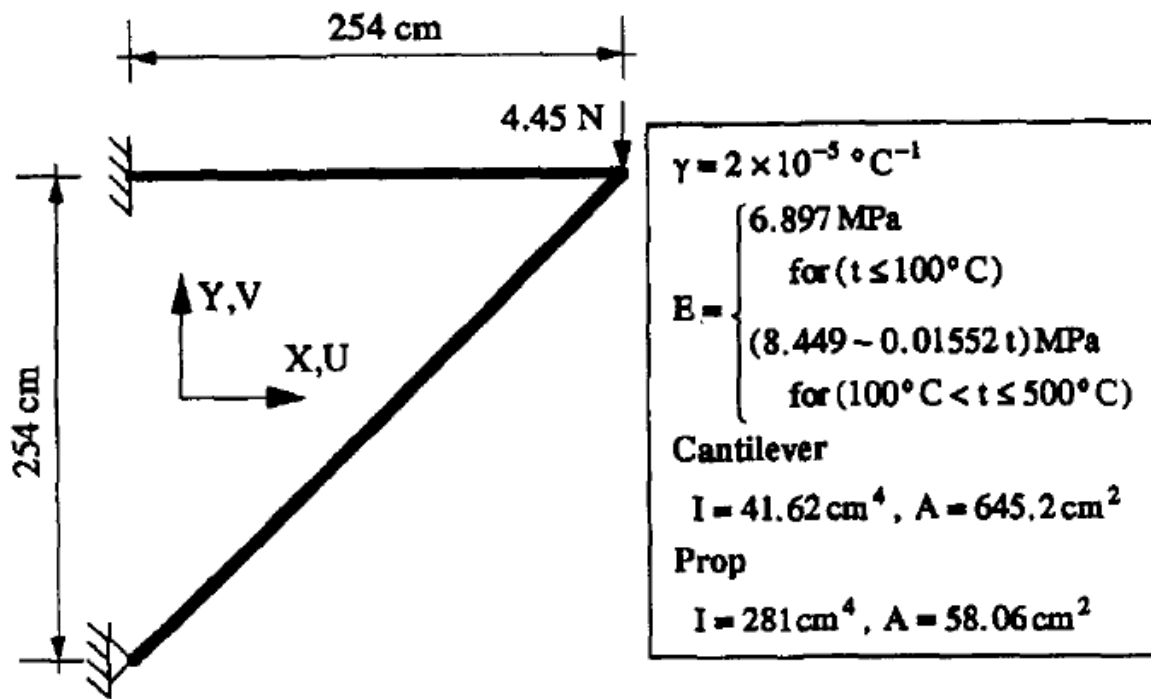


Fig. 11 Geometric configuration of propped cantilever

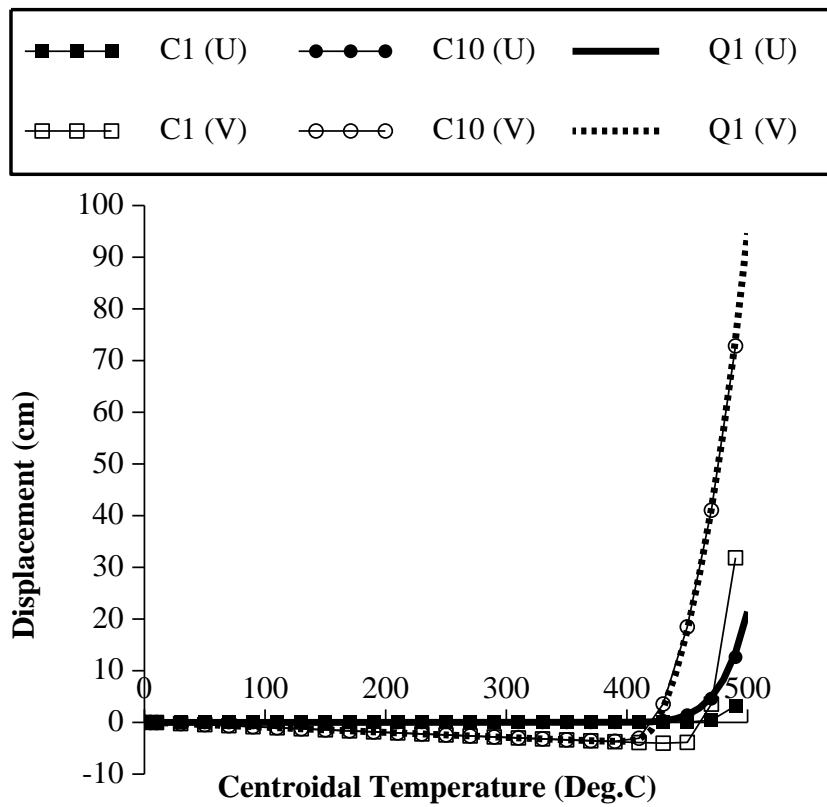


Fig. 12.a Buckling of propped cantilever: tip displacements

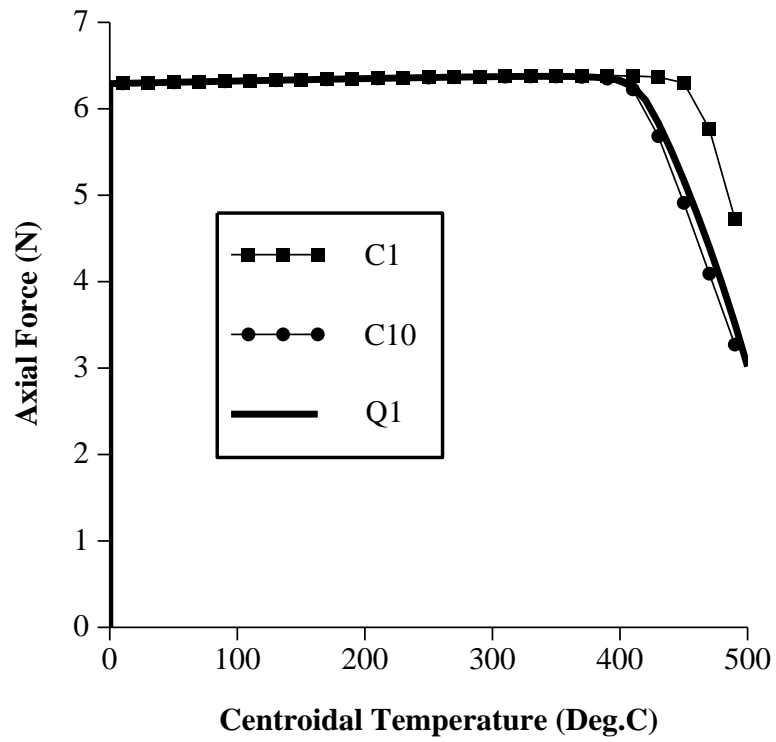


Fig. 12.b Buckling of propped cantilever: prop axial force

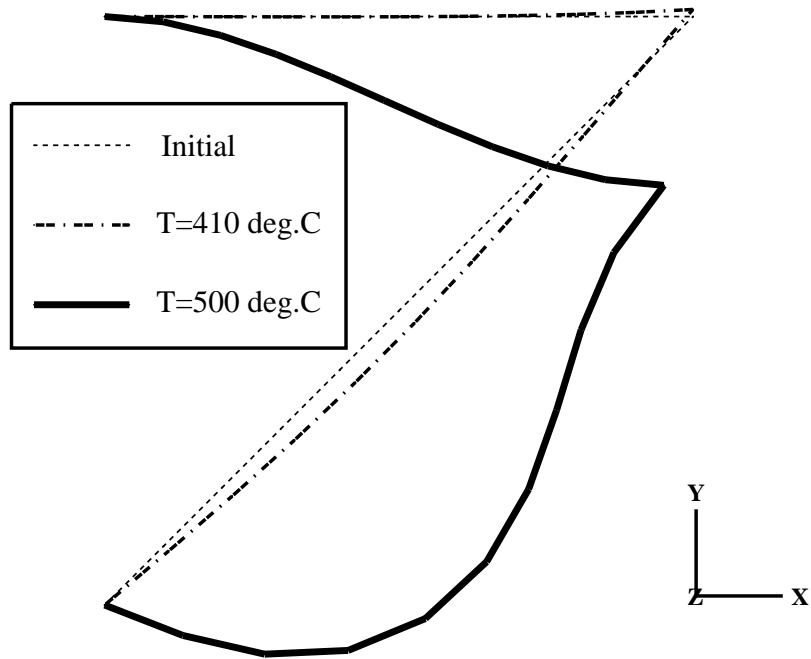


Fig. 13 Deflected shapes of propped cantilever